

Optimization analysis of a double-steady-state clutch for hybrid electric vehicles

QING-YONG ZHANG², CHANG-LUN WU³, JIAN HUANG^{2,3}

Abstract. The mode switch of hybrid electric vehicles between internal combustion engines and motors is essential to vehicle's power and drivability performance. Due to the different working conditions in hybrid electric buses compared with traditional vehicles, it is critical to analyze main clutch and its key parts. The main objective of this paper is to investigate the optimal design of a double-steady-state clutch applied on electric hybrid buses. The rotating reinforcement clutch was introduced and its structure was analyzed. The principle of optimal design was described and the method of Goal Driven Optimization was applied to the parameters of a double-steady-state clutch. The rear end cover and the king pin of the clutch were modeling and optimal design was executed. Simulation results reveal that the key parameters of the rear end cover and the king pin have been improved.

Key words. Main clutch, double-steady-state clutch, goal driven optimization, parameter sensitivity.

1. Introduction

Main clutch exists as an independent assembly in the power train of hybrid electric vehicles. At present, friction clutch is widely applied in different types of hybrid electric vehicles[1]. Running of hybrid electric vehicles requires continuous switchover of different drive modes and each switchover is accomplished through separating and engaging of clutch. This differs from traditional vehicles significantly[2][3]. Compared to traditional vehicles, hybrid electric vehicles have longer

¹Acknowledgment - This project is supported by the project grant from natural science foundation of Fujian province(2015J01179), the projects of technological innovation and strategic emerging industries of Fujian provincial economic and trade commission, the projects of industry-university collaboration of Fuzhou municipal economic and trade commission.

²Workshop 1 - School of Mechanical and Automotive Engineering, Fujian University of Technology, 350118, China

³Workshop 2 - Fujian Wanrun New Energy Technology Co., Ltd, 350108, China

time for the clutch being separated and thereby longer time of keeping the release bearing pressed. The pressing force on the release bearing is acting on the flywheel and finally transmits to bent axle of the engine. The bent axle of the engine will suffer a strong axial pressing force for a long time, which will affect the engine performance significantly[4]. Nowadays, main clutch failure becomes one primary technical bottleneck of hybrid electric vehicles[5].

Main clutch control in hybrid electric vehicles in China mainly uses cylinder driven control for the moment[6]. Many additional parts have been added to meet working conditions of clutch in hybrid electric vehicles, which leads to the highly complicated control mechanism of the whole clutch and brings a series of problems[7][8].

The clutch control strategy in parallel hybrid electric vehicles was studied, finding they used the combined control strategy of a synchronized engaging and a launch slip engaging maneuver. It also designed a learning algorithm for clutch compensation[2].

2. Configuration and working principle for double-steady-state clutches

2.1. Propose of the double-steady-state clutch

There are two working modes of the clutch: long-term engaging and long-term separated. The vehicle clutch running at one mode for a long time is called mono-steady-state clutch and the vehicle clutching running at two modes for a long time as double-steady-state clutch. Most clutches used in vehicle in China are mono-steady-state clutch. According to driving characteristics of hybrid electric vehicles, it requires a double-steady-state clutch rather than a mono-steady-state clutch. However, there's no double-steady-state clutch available on the Chinese market. Design and theory of double-steady-state clutch haven't been studied yet. With the increase of hybrid electric vehicles, studying double-steady-state clutch has important significance to meet requirements.

2.2. Rotating reinforcement clutch

Structure of an electromagnetism-driven rotating reinforcement clutch is shown in Fig.1. As an open double-steady-state clutch, holes on the front rotating platen form loose fit with the king pin, so the front rotating platen can make free slides axially on the king pin. The return spring is between the flywheel and the front rotating platen and has certain preload, which can ensure that the front rotating platen, steel ball and back rotating platen pressed onto the needle roller thrust bearing and adjoin to the rear end cover of the clutch. The Auxiliary pin head is fixed onto the driving part of the assistant clutch. The hinge pin forms loose fit with holes on the back rotating platen, so the driven disc is free to slide on the slave spline shaft.

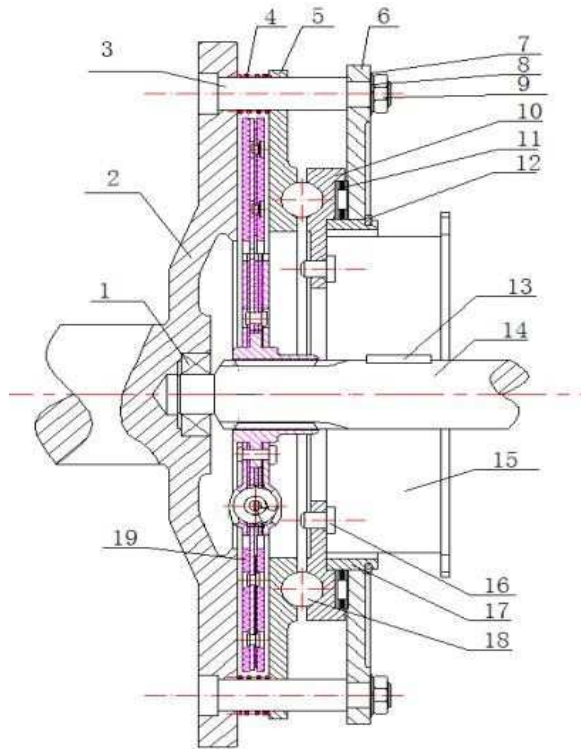


Fig. 1. Structure of an electromagnetism-driven rotating reinforcement clutch

3. Optimization of some parts of double-steady-state clutch

3.1. Theory of optimization design

Optimization design is to get the optimal design plan by establishing an optimization model, determining design variables, objective function and constraints, using different optimization approaches, and calculating the optimal value of the objective function through multiple iterations[9].

$$(1) \quad \text{The optimization mathematical model: } \begin{cases} \min F(X) = F(x_1, x_2, \dots, x_n) \\ g_i(X) = g_i(x_1, x_2, \dots, x_n), i = 1, 2, \dots, M \\ X = (x_1, x_2, \dots, x_n)^T \end{cases}$$

Design variables are independent variables and the optimization is realized by changing numerical values of design variables. Every design variable has upper and lower limits. State variables are numerical values that restrict design. They are the function of design variables. They may have upper and lower limits. The objective function is a numerical value as small as possible and is the function of design variables.

3.2. Numerical simulation analysis of rear end cover

First, parameters of the rear end cover model were set. Three thickness (hou1=1mm, hou2=9mm and hou3=2mm) of the rear end cover were set as the design input variables. Next, structural static mechanics were analyzed, which concluded that the minimum stress safety factor was 2.39. Stress safety factor was set as the output variable (Fig.2). At this moment, mass of the rear end cover was 8Kg.

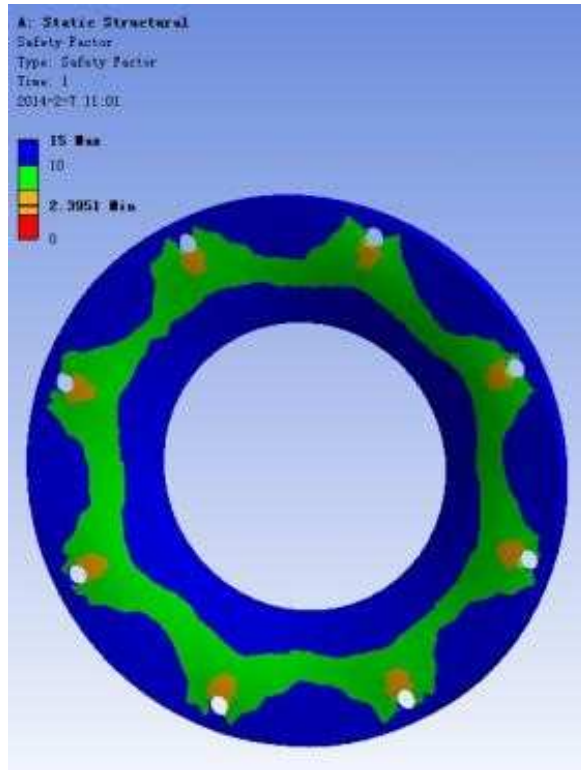


Fig. 2. Cloud chart of stress safety factor

This paper adopted Goal Driven Optimization. This module was dragged into the optimization flowchart, which would connect with the parameter space produced by structural static mechanics automatically (Fig.3). In the experimental design, optimization ranges of input design variables were set: 0.1mm ~ 2mm for hou1, 3mm ~ 10mm for hou2, and 1mm ~ 5mm for hou3.

Design sample points that meet the parameter ranges in the point table and update design of experiments. Calculated results of sample design points gained from the program running are shown in Fig.4.

Update the Response Surface and get values of input parameters corresponding to the maximum and minimum output parameters. The search results are shown in Fig.5.

Goodness of fit on the Response Surface is checked. Sensitivity graph reflects

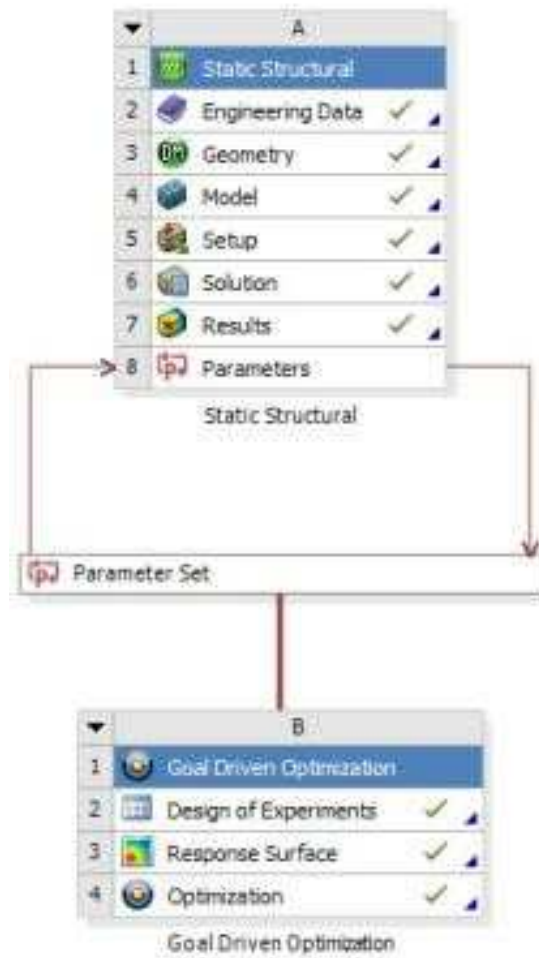


Fig. 3. Optimization flowchart

| Table of Schematic B2: Design of Experiments | | | | | | |
|--|------|-----------|-----------|-----------|-------------------------|----------------------------|
| A | B | C | D | E | F | |
| 1 | Name | P1 - hou1 | P2 - hou2 | P3 - hou3 | P4 - Geometry Mass (kg) | P5 - Safety Factor Minimum |
| 2 | 1 | 1.05 | 6.5 | 3 | 6.495 | 1.9553 |
| 3 | 2 | 0.1 | 6.5 | 3 | 5.9203 | 1.717 |
| 4 | 3 | 2 | 6.5 | 3 | 7.0696 | 2.3915 |
| 5 | 4 | 1.05 | 3 | 3 | 3.8779 | 0.96561 |
| 6 | 5 | 1.05 | 10 | 3 | 9.112 | 3.3783 |
| 7 | 6 | 1.05 | 6.5 | 1 | 5.8286 | 1.1351 |
| 8 | 7 | 1.05 | 6.5 | 5 | 7.1614 | 2.8169 |
| 9 | 8 | 0.27762 | 3.6544 | 1.3739 | 3.3582 | 0.52532 |
| 10 | 9 | 1.8224 | 3.6544 | 1.3739 | 4.2926 | 0.81151 |
| 11 | 10 | 0.27762 | 9.3456 | 1.3739 | 7.6137 | 1.9176 |
| 12 | 11 | 1.8224 | 9.3456 | 1.3739 | 8.5481 | 2.5119 |
| 13 | 12 | 0.27762 | 3.6544 | 4.6261 | 4.4418 | 1.3102 |
| 14 | 13 | 1.8224 | 3.6544 | 4.6261 | 5.3762 | 1.9141 |
| 15 | 14 | 0.27762 | 9.3456 | 4.6261 | 8.6973 | 3.6139 |
| 16 | 15 | 1.8224 | 9.3456 | 4.6261 | 9.6317 | 4.3445 |

Fig. 4. Sample design points generated by design of experiments

| Table of Outline A12: Min-Max Search | | | | | | |
|--------------------------------------|---|-----------|-----------|-----------|------------------------|----------------------------|
| | A | B | C | D | E | F |
| 1 | Name | P1 - hou1 | P2 - hou2 | P3 - hou3 | P4 - Geometry Mass (g) | P5 - Safety Factor Minimum |
| 2 | Output Parameter Minimums | | | | | |
| 3 | P4 - Geometry Mass Minimum Design Point | 0.1 | 3 | 1 | 2.6369 | 0.32082 |
| 4 | P5 - Safety Factor Minimum Minimum Design Point | 0.1 | 3 | 1 | 2.6369 | 0.32082 |
| 5 | Output Parameter Maximums | | | | | |
| 6 | P4 - Geometry Mass Maximum Design Point | 2 | 10 | 5 | 10.353 | 5.0086 |
| 7 | P5 - Safety Factor Minimum Maximum Design Point | 2 | 10 | 5 | 10.353 | 5.0086 |

Fig. 5. Search map of maximum and minimum

sensitivities of design points to output parameters. It can be known from Fig.6 that hou2 influences deformation mostly. The variation of an input parameter with another one or more input parameters can be observed by changing values of design points.

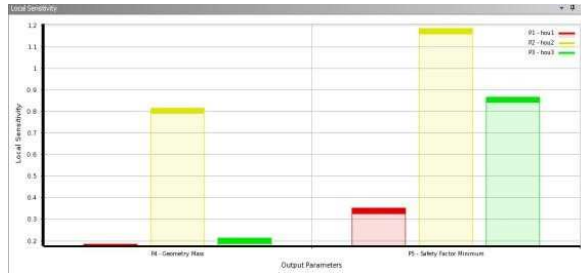


Fig. 6. Parameter sensitivity observation at response points

Results on the Response Surface are shown on Fig.7~Fig.12.

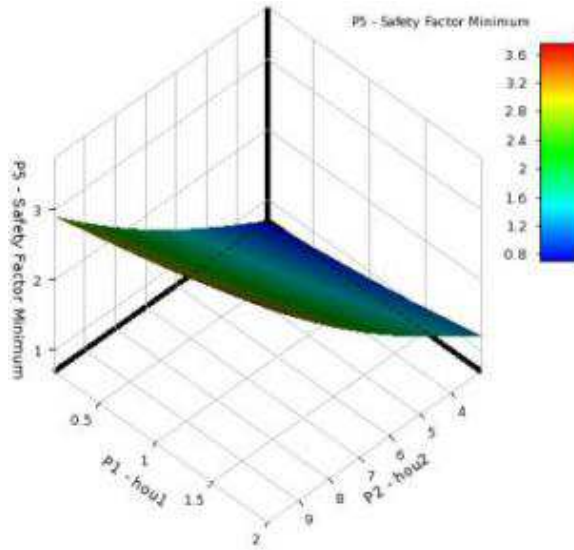


Fig. 7. Response surface of safety factor to hou1 and hou2

In the optimization unit, mass was set as the optimization goal and minimum stress safety factor was set ≥ 1.2 . Update the optimization and generate 1,000 sample

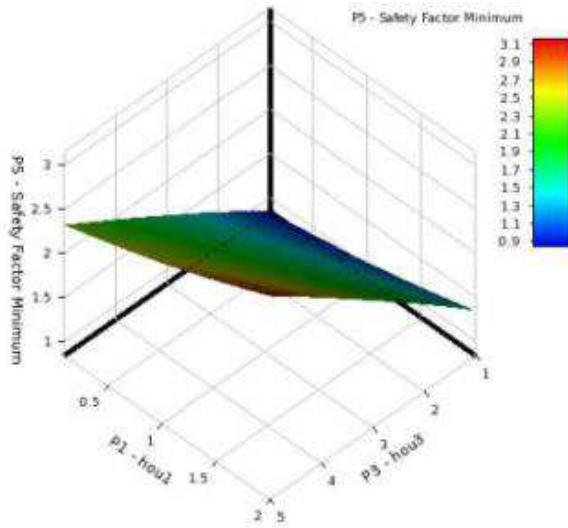


Fig. 8. Response surface of safety factor to hou1and hou3

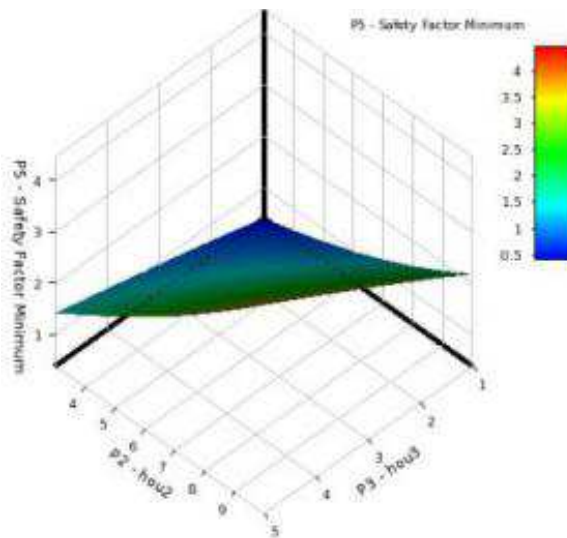


Fig. 9. Response surface of safety factor to hou2 and hou2

points by using the Response Surface. Finally, the program gave three best results (Fig.13).

It can be known from Fig.13 that hou1 can be simplified to 0mm, while hou2 and hou3 can be determined 4.8mm and 3.7mm, respectively.

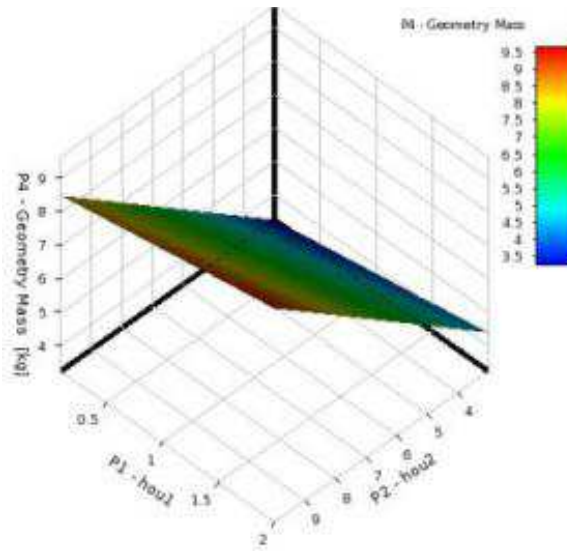


Fig. 10. Response surface of mass to hou1 and hou2

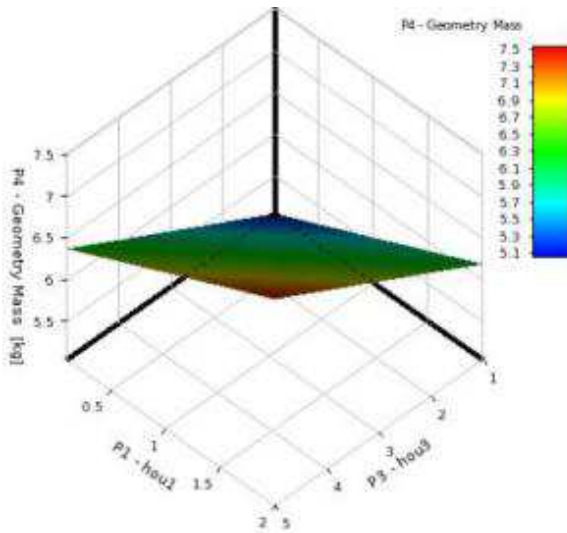


Fig. 11. Response surface of safety factor to hou1 and hou3

3.3. Numerical simulation analysis of kingpin

Three cylinder diameters and one base angle thickness of the king pin were used as input variables: zhijing1 (z_1)=26mm, zhijing2 (z_2)=20mm, zhijing3 (z_3)=16mm and hou1=7mm. Next, structural static mechanics were analyzed, which concluded that the minimum stress safety factor was 4.36. Stress safety factor was set as the output variable. At this moment, mass of the king pin was 0.22Kg.

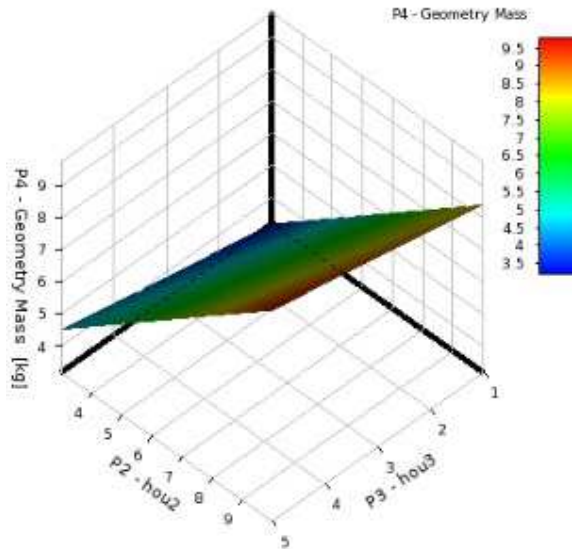


Fig. 12. Response surface of mass to hou2 and hou3

| Table of Schematic B/F: Optimization | | | | | | |
|--------------------------------------|--------------------|--------------|--------------|--------------|-------------------------|----------------------------|
| | A | B | C | D | E | F |
| 1 | | P1 - hou1 | P2 - hou2 | P3 - hou3 | P4 - Geometry Mass (kg) | P5 - Safety Factor Minimum |
| 2 | Optimization Study | | | | | |
| 3 | Objective | No Objective | No Objective | No Objective | No Objective | Values >= Target |
| 4 | Target Value | | | | | 1.2 |
| 5 | Importance | Default | Default | Default | Default | Default |
| 6 | Candidate Points | | | | | |
| 7 | Candidate A | 0.10285 | 6.5035 | 2.3353 | 5.7032 | 1.4494 |
| 8 | Candidate B | 0.10475 | 4.7535 | 3.6687 | 4.8401 | 1.3849 |
| 9 | Candidate C | 0.11425 | 9.1285 | 3.2242 | 7.9691 | ★ 2.76 |

Fig. 13. Optimization results

Design Driven Optimization was used in this optimization. This module was dragged into the optimization flowchart, which would connect with the parameter space produced by structural static mechanics automatically. In the experimental design, optimization ranges of input design variables were set: 22mm ~ 30mm for zhijing1, 12mm ~ 22mm for zhijing2, 8mm ~ 16mm for zhijing3, and 4mm ~ 10mm for hou1.

Preview Design of Experiments, design sample points that meet the parameter ranges in the point Table and Update Design of Experiments. Update the Response Surface and choose Min-Max Search in output parameters. The attribute window can set Number of Initial Surface as 100 and Number of start surface as 3. Thus getting values of input parameters corresponding to maximum and minimum output parameters.

Goodness of fit on the Response Surface is checked. Sensitivity graph reflects sensitivities of design points to output parameters. The variation of an input parameter with another one or more input parameters can be observed by changing values of design points, shown in Fig.14.

Results on the Response Surface of safety factor to zj1 and zj2, safety factor to

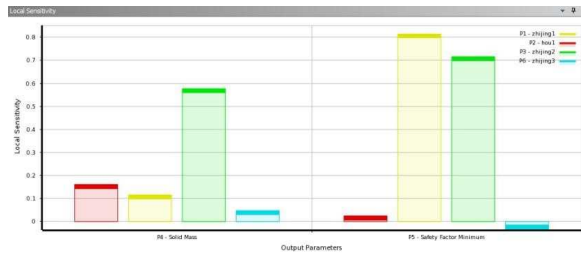


Fig. 14. Parameter sensitivity observation at response points

zj1 and zj3, safety factor to zj1 and hou1, mass to zj2 and zj3, mass to zj2 and hou1 and mass to zj2 and hou1 are checked.

In the optimization unit, mass was set as the optimization goal and minimum stress safety factor was set 1.5. Update the optimization and generate 1,000 sample points by using the Response Surface. Finally, the program gave three best results (Fig. 15).

| Table of Schematic 04: Optimization | | | | | | | |
|-------------------------------------|--------------------|--------------|--------------|--------------|--------------|----------------------|----------------------------|
| | A | B | C | D | E | F | G |
| 1 | | P2 - hou1 | P1 - zhjing1 | P3 - zhjing2 | P6 - zhjing3 | P4 - Solid Mass (kg) | P5 - Safety Factor Minimum |
| 2 | Optimization Study | | | | | | |
| 3 | Objective | No Objective | No Objective | No Objective | No Objective | No Objective | Values >= Target |
| 4 | Target Value | | | | | | 1.5 |
| 5 | Importance | Default | Default | Default | Default | Default | Default |
| 6 | Candidate Points | | | | | | |
| 7 | Candidate A | → 4.009 | → 26.004 | → 14.671 | → 8.802 | → 0.1262 | ★ 3.9584 |
| 8 | Candidate B | → 4.015 | → 24.004 | → 17.337 | → 9.602 | → 0.15546 | ★★ 4.6049 |
| 9 | Candidate C | → 4.039 | → 25.004 | → 13.782 | → 8.962 | → 0.11635 | ★ 3.506 |

Fig. 15. Optimization results

It can be known from Fig.15 that when hou1=4mm, zhijing1, zhijing2 and zhijing3 are 25mm, 13.8mm and 9mm, respectively. The mass of kingpin was 0.116kg.

4. Conclusion

In this work, a double-steady-state clutch for hybrid electric vehicles were exploited. The detailed structure of a rotating reinforcement clutch for hybrid electric buses was described. The method optimal design and the flowchart of numerical optimization were introduced. The method of design driven optimization was applied to optimize the rear end cover and the king pin. Search results, goodness of fit and parameter sensitivity on the Response Surface of the rear end cover and the king pin were checked respectively. Goal driven optimization results was obtained and that shows the key parameters of the rear end cover and the king pin were optimized. Future work includes more compact system design combined with the clutch actuator and system optimization. In the future research, we will integrate the transmission systems with engine and vehicle control.

References

- [1] K. MINKUK, K. HYUNJUN, K. DONGSUK: *Systematic configuration selection methodology of power-split hybrid electric vehicles with a single planetary gear*. Proceedings of the ASME 2014 Dynamic Systems and Control Conference 10 (2014) 211–220.
- [2] C. Q. NI, Y. K.T. ZHANG, Q. ZHAO, A. BOUKEHILI: *Dynamic torque control strategy of engine clutch in hybrid electric vehicle*. Journal of mechanical engineering 49 (2013) 114–121.
- [3] M. G. TEHRANI, J. MONTONEN, P. IMMONEN, ETC: *Application Of Hub-Wheel Electric Motor Integrated With Two Step Planetary Transmission For Heavy Off-Road Vehicles*. Proceedings of the ASME 2015 International Design Engineering Technical Conferences & Computers and Information in Engineering Conference 8 (2015) 1–8.
- [4] E. GALVAGNO, D. MORINA, A. SORNIOTTI, M. VELARDO-CHIA: *Drivability analysis of through-the-road-parallel hybrid vehicles*. Meccanica 48 (2013) 351–366.
- [5] Z. WEI, X. GUO: *Analysis and modeling of transmission efficiency of vehicle driveline*. SAE International, January (2014).
- [6] J. PARK: *Development of Engine Clutch Control for Parallel Hybrid Vehicles*. World Electric Vehicle Journal 6 (2013) 283–287.
- [7] L. WALTER, T. ROCHDI, D. PHILIPPE, ETC: *Switched Causal Modeling of Transmission With Clutch in Hybrid Electric Vehicles*. Ieee transactions on vehicular technology 57 (2008) 2081–2088.
- [8] X. ZHOU, P. WALKER, N. ZHANG: *Study of power losses in a two-speed dual clutch transmission*. SAE Technical papers 1 (2014).
- [9] L. LI, H. ZHAO, Y. WANG: *MDO Approach for Frictional Electromagnetic Clutch Design*. Journal of System Simulation 24 (2012) 314–317.

Received November 16, 2016

